Hydrodynamics of Fluidization: Prediction of Wall to Bed Heat Transfer Coefficients

A computer model for a hot fluidized bed was developed. The large heat transfer coefficients characteristic of fluidized beds were computed without an enhancement of heat transfer by turbulence. They agreed with measurements reported by Ozkaynak and Chen (1980) within the accuracy of estimated thermal conductivity of solids.

M. SYAMLAL and DIMITRI GIDASPOW

Illinois Institute of Technology
Department of Chemical Engineering
Chicago, IL 60616

SCOPE

Fluidized beds are ideal for gasifying coal due to high rates of heat and mass transfer and solids mobility. Environmental constraints make them also very useful for coal combustion to produce electric power. However, one of the largest concerns when using fluidized beds to commercialize many chemical processes is scale-up. We believe this is due to the absence of an experimentally verified hydrodynamic theory that can describe the complicated transient gas and solid motion in a fluid bed. During the past few years several organizations began to develop hydrodynamic computer models that promise to be predictive in many respects. In the area of gasification a workshop chaired by Ghate and Martin (1982) summarized the models developed by the Systems, Science and Software group (Schneyer et al., 1981) and by the JAYCOR group (Scharff et al., 1982). For fluidized bed combustion, the model by Adams and Welty (1979) proved to be very useful for explaining heat transfer coefficients from a horizontal tube to a fluidized bed. A cold fluidized bed model developed at Illinois Institute of Technology (IIT) (Gidaspow, et al., 1983; Ettehadieh, 1982) for a two-dimensional bed was able to predict void distributions, solids circulation, and bubbling behaviors. A critical test for a fluidized bed hydrodynamic model, is its ability to predict the experimentally observed large heat transfer coefficients.

CONCLUSIONS AND SIGNIFICANCE

The IIT model was extended to a heated fluidized bed. Our results suggest that in a bubbling bed the large heat transfer coefficients can be computed from our hydrodynamic model without the use of any turbulence as used in the model of Klein and Scharff (1982). The model itself computes a transient type behavior caused by the formation of bubbles, their propagation, and eruption at the top of the bed. All the computed variables, the void fraction, the gas and solid velocities, and the temperatures undergo a complex oscillatory behavior.

This model should be useful for studying effects of reactor configurations and for making parametric studies for process optimization.

INTRODUCTION

Fluidized beds find application as excellent heat transfer media. The transition to fluidized state is accompanied by a remarkable increase in the bed-to-wall heat transfer coefficient. Such a drastic change is a result of the peculiar hydrodynamics in the fluidized state. Thus it has been a subject of intense investigation for the past several years. A review of these studies may be found in Gelperin and Einstein (1971), Botterill (1975), and Saxena et al. (1978).

The complexity of the heat transfer phenomena in the fluidized state is attested by the large number of correlations available for computing the heat transfer coefficient. But these formulae are valid only within the limits of the experimental conditions on which they are based, and may differ by almost two orders of magnitude from the actual coefficients in some cases (Gelperin and Einstein, 1971). Hence, the investigators are motivated to study the mechanism of heat transfer more closely.

From the early 1950s, investigators started proposing mechanistic models for predicting the heat transfer coefficient. As pointed out by Gelperin and Einstein (1971), these models may be broadly classified as follows, on the basis of the dominating mechanism:

1. Models based on conductive heat transfer through the fluid boundary layer near the heat transfer surface. These models have the major drawback of neglecting the thermal-physical properties of the solid.
2. Models using the assumption that the dominant part in transferring the heat is played by the solids. These models are unsuitable for gas fluidized beds.
3. Models based on the postulate that heat is transferred by "packets" of solids which are periodically replaced from the heat transfer surface by gas bubbles. This mechanism breaks down for ϵ greater than 0.7.

The last mechanism, originally due to Mickley and Fairbanks, has been extensively used in various modified forms. Later in this work we will find that the "packet" model is in some respects similar to the continuum approach developed here.

TABLE 1. HYDRODYNAMIC MODEL

Continuity Equations

Gas Phase

$$\frac{\partial}{\partial t}(\rho_g \epsilon) + \frac{\partial}{\partial x}(\epsilon \rho_g U_g) + \frac{\partial}{\partial y}(\epsilon \rho_g V_g) = 0$$

Solid Phase

$$\frac{\partial}{\partial t}[\rho_s(1-\epsilon)] + \frac{\partial}{\partial x}[\rho_s U_s(1-\epsilon)] + \frac{\partial}{\partial y}[\rho_s(1-\epsilon)V_s] = 0$$

Momentum Equations

Gas Momentum in x Direction

$$\frac{\partial}{\partial t}(\rho_g \epsilon U_g) + \frac{\partial}{\partial x}(\rho_g \epsilon U_g U_g) + \frac{\partial}{\partial y}(\rho_g \epsilon V_g U_g) = -\epsilon \frac{\partial P}{\partial x} + \beta_x(U_s - U_g)$$

Solids Momentum in x Direction

$$\frac{\partial}{\partial t}[\rho_s(1-\epsilon)U_s] + \frac{\partial}{\partial x}[\rho_s(1-\epsilon)U_s U_s] + \frac{\partial}{\partial y}[\rho_s(1-\epsilon)V_s U_s] = -(1-\epsilon)\frac{\partial P}{\partial x} + \beta_x(U_g - U_s) - \frac{\partial \tau}{\partial x}$$

Gas Momentum in y Direction

$$\frac{\partial}{\partial t}(\rho_g \epsilon V_g) + \frac{\partial}{\partial x}(\rho_g \epsilon U_g V_g) + \frac{\partial}{\partial y}(\rho_g \epsilon V_g V_g) = -\epsilon \frac{\partial P}{\partial y} + \beta_y(V_s - V_g) - \rho_g \epsilon g$$

Solids Momentum in y Direction

$$\frac{\partial}{\partial t}[\rho_s(1-\epsilon)V_s] + \frac{\partial}{\partial x}[\rho_s(1-\epsilon)U_s V_s] + \frac{\partial}{\partial y}[\rho_s(1-\epsilon)V_s V_s] = -(1-\epsilon)\frac{\partial P}{\partial y} + \beta_y(V_g - V_s) - \rho_s(1-\epsilon)g - \frac{\partial \tau}{\partial y}$$

The packet model gives the local instantaneous heat transfer coefficient in terms of a penetration mechanism as:

$$h_i = \left(\frac{k_a \rho_b C_s}{\pi \tau_p}\right)^{1/2} \tag{1}$$

Here, τ_p is the time for which the packet was in contact with the heat transfer surface. Although such detailed models describe the means by which surface-to-bed heat transfer takes place, they are of limited application because they require a knowledge of parameters which are not easily available (Botterill, 1975; Ozkaynak and Chen, 1980).

For large-particle fluidized beds, a gas convection model of heat transfer was proposed by Adams and Welty (1979). In their work, the heat transfer from a horizontal tube is modeled using boundary layer equations for the gas phase. The average interstitial gas velocity is calculated from an approximate analytical solution of the two-phase flow equations. The mechanism of heat conduction to the solid phase is neglected. A transfer mechanism by means of turbulence is introduced. Such a mechanism was earlier used by Galloway and Sage (1970). The particle sizes used in both of the studies mentioned above are about an order of magnitude larger than those considered here.

Since the advent of high-speed computers, there have been attempts by several organizations—Systems, Science and Software, JAYCOR, and IIT—to model the fluidized bed using a continuum approach. As an example, Gidaspow and Ettehadieh (1983) recently demonstrated that the hydrodynamics in a two-dimensional fluidized bed may be described by a set of two-phase flow equations. In such a formulation the solid particles are represented as a continuous particulate phase. This approximation is valid due to the relatively small size of the individual solid particles in comparison to the bed dimensions.

HYDRODYNAMIC MODEL

Hydrodynamic models of fluidization use the principles of conservation of mass, momentum and energy. Table 1 shows the continuity and the separate phase momentum equations for two-dimensional transient two-phase flow. There are six nonlinear coupled partial differential equations for six dependent variables. The variables to be computed are the void fraction ϵ, the pressure P, the gas velocity components U_g and V_g, and the solids velocity components U_s and V_s, in the x and y directions, respectively. The equations are written in a form found in the K-FIX computer code (Rivard and Torrey, 1977) for gas-liquid flow. The sum of the solids and the gas momentum equations gives the mixture momentum equations. These mixture momentum equations and the continuity equations are generally accepted by the majority of two-phase flow investigators. However, the presence of the gradient of pressure in the solid momentum equations makes the initial value problem ill-posed, as discussed in detail by Lyczkowski et al. (1978). This leads to an unstable solution. To overcome this problem, a normal component of solids stress, sometimes associated with solids pressure or particle to particle interaction is kept in the K-FIX equations. Stresses associated with gas and solids viscosities have been deleted. The numerical value of the stress used is very small. In addition to helping stability, this extra force keeps the particles from collapsing to unreasonably low gas volume fractions, similar to that in the hydrodynamic model of Pritchett et al. (1978). However, unlike the Garg and Pritchett model (1975), the hydrodynamic model has only one major empirical input. It is the well-accepted drag correlation, given by β. Garg and Pritchett also do not use the momentum equation for the gas in the form shown in Table 1. They use Darcy's law in its place. However, at this level of accuracy, differences between investigators are beginning to appear. For example, Gidaspow (1978) cured the ill-posedness problem by deriving a relative velocity equation using non-equilibrium thermodynamics. Arastoopour and Gidaspow (1979) compared the numerical results of three hydrodynamic models for pneumatic transport and found them to be very similar. The drag correlation has such a large effect that it dampens difference between the models, once one uses the same mixture momentum equations. In view of this the K-FIX model properly stabilized is a reasonable model for two phase flow calculations. The boundary conditions (BC) used are as follows:

BC1: At $y = 0$ we have $\rho_g V_g = C_j$; that is, we prescribe a constant gas mass flux through the distributor plate.

BC2: At $y = L$, we have P = atmospheric and $V_s = 0$; that is, we have a wire mesh to prevent solid carry-over from bed.

BC3: At $x = 0$, $U_s = U_g = 0$, and $V_g = 0$; that is, we have a solid wall with no slip.

BC4: At $x = W$, $U_s = U_g = 0$, and $V_g = 0$; that is, we have a solid wall with no slip.

The initial condition is assumed to be that of minimum fluidization.

The space above the dense portion of the fluid bed, called the free board, is of the same size as the initial bed height and is provided to allow for bed expansion. At time zero the gas flow rate is increased. Figure 1 shows the bed dimensions, the typical particle diameter, and the other data used in the numerical calculations reported here.

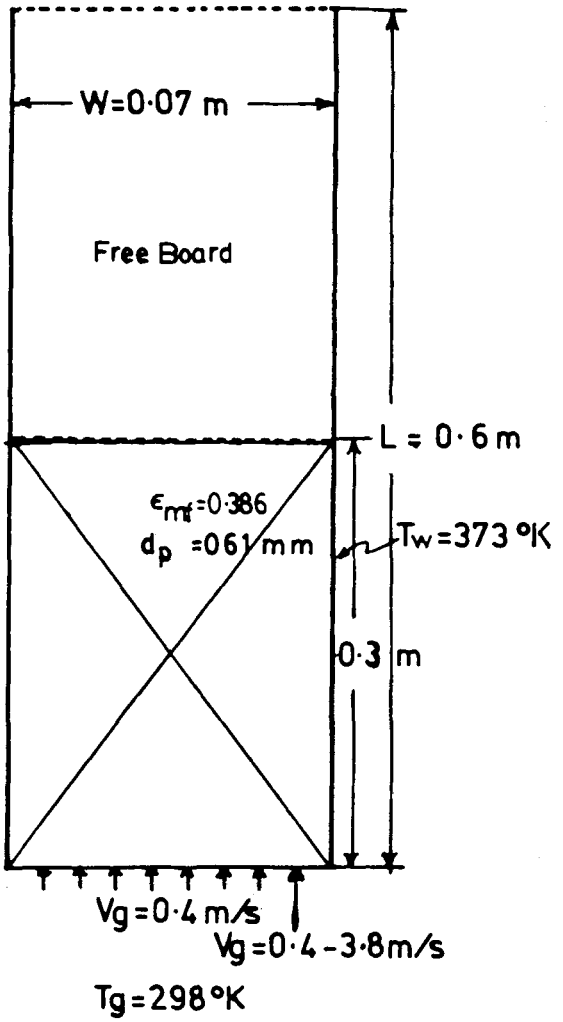

Figure 1. Typical data for numerical computations.

Fluid Particle Drag

The major empirical input in this cold bed model is the fluid-particle coefficient, β. It is obtained from standard correlations as follows.

According to Wen and Yu (1971), for porosities less than 0.8 the pressure drop due to friction between gas and solids can be described by the Ergun equation. Thus the friction coefficient in this porosity range becomes,

$$\beta_y = 150\frac{(1-\epsilon)^2\mu_g}{\epsilon(d_p\phi_s)^2} + 1.75\frac{\rho_g|V_g - V_s|(1-\epsilon)}{\phi_s d_p} \tag{2}$$

Rietma and Mutsers (1973) have also found a similar expression for β whose reciprocal they call mobility.

Wen and Yu (1965) have extended the works of Richardson and Zaki (1954) to derive an expression for pressure drop prediction in particulate beds. For porosities greater than 0.8 such a relation for pressure drop leads to the following expression for the friction coefficient.

$$\beta_y = \frac{3}{4}C_{dy}\frac{\epsilon(1-\epsilon)|V_g - V_s|\rho_g}{d_p\phi_s}f(\epsilon), \quad \epsilon \geq 0.8 \tag{3}$$

where C_{dy}, the drag coefficient in y direction, is related to Reynolds number (Rowe, 1961).

$$C_{Dy} = \frac{24}{Re_{sy}}(1 + 0.15Re_{sy}^{0.687}), \quad Re_{sy} < 1{,}000 \tag{4}$$

$$C_{Dy} = 0.44 \quad Re_{sy} \geq 1{,}000 \tag{5}$$

where

$$Re_{sy} = \frac{\rho_g(V_g - V_s)d_p}{\mu_g} \tag{6}$$

In Eq. 3 $f(\epsilon)$ shows the effect due to the presence of other particles in the fluid and acts as a correction to the usual Stokes law for free fall of a single particle. We use

$$f(\epsilon) = \epsilon^{-2.65} \tag{7}$$

The expression for the friction coefficient in the x direction is the same as that in the axial direction, y.

Solids Stress

In a general formulation the solids momentum equations would contain solids stress terms that are a function of porosity, pressure, and the displacement tensors of solids velocity, gas velocity, and relative velocity. Such a general formulation with proper values of material constants does not exist today. However, as already described, it is necessary to use the normal component of the solids stress to prevent the particles from reaching impossibly low values of void fraction. Rietma and Mutsers (1973) have introduced such a term into fluidization modeling and have made measurements. Measurements of such a stress for settling showed it to be quite small compared with the hydrostatic pressure. In view of the previous theory and measurements, the constitutive equation for the normal component of the stress τ is

$$\tau = \tau(\epsilon)$$

Then by chain rule,

$$\frac{\partial\tau}{\partial y} = \frac{\partial\tau}{\partial\epsilon}\cdot\frac{\partial\epsilon}{\partial y} \tag{8}$$

Using the nomenclature of Pritchett et al (1978), let the modulus of elasticity or particle-to-particle interaction coefficient be

$$G(\epsilon) = \frac{\partial\tau}{\partial\epsilon} \tag{9}$$

In this study this modulus is fitted to the experimental data of Rietma and Mutsers (1973) by the equation

$$-G(\epsilon) = 10^{(-8.76\epsilon+5.43)}, \quad \mathrm{N/m^2} \tag{10}$$

This term becomes of numerical significance only when the void fractions go below the minimum fluidization void fraction. It also helps to make the system numerically stable, because it converts the imaginary characteristics into real values.

Fanucci, Ness, and Yen (1979) have obtained the characteristic directions for one-dimensional incompressible flow for the set of equations shown in Table 1. Their paper shows one of their characteristics, C, to be

$$C = \left[\frac{1}{\rho_g/\epsilon + \rho_s/\epsilon_s}\right]^{1/2}\left[\frac{-(V_g - V_s)^2}{\epsilon/\rho_g + \epsilon_s/\rho_s} - \frac{G(\epsilon)}{\epsilon_s}\right]^{1/2} \tag{11}$$

The above relation shows that as the void fraction goes to zero, $-G(\epsilon)$ becomes large and makes the characteristics real. In practice we find that this extra stress permits us to continue calculations in time without a loss of material balance. Without this term, the K-FIX code gave results that showed a loss of mass after about 0.7 seconds of operation even with a very strict convergence criterion.

ENERGY EQUATIONS

The energy equations are also written in a form found in the K-FIX computer code (Rivard and Torrey, 1977) as given below:

$$\frac{\partial}{\partial t}(\epsilon\rho_g I_g) + \frac{\partial}{\partial x}(\epsilon\rho_g I_g U_g) + \frac{\partial}{\partial y}(\epsilon\rho_g I_g V_g)$$
$$= -P\left[\frac{\partial\epsilon}{\partial t} + \frac{\partial}{\partial x}(\epsilon U_g) + \frac{\partial}{\partial y}(\epsilon V_g)\right] + h_v(T_s - T_g)$$
$$+ \frac{\partial}{\partial x}\left(K_g\epsilon\frac{\partial T_g}{\partial x}\right) + \frac{\partial}{\partial y}\left(K_g\epsilon\frac{\partial T_g}{\partial y}\right) \tag{12}$$

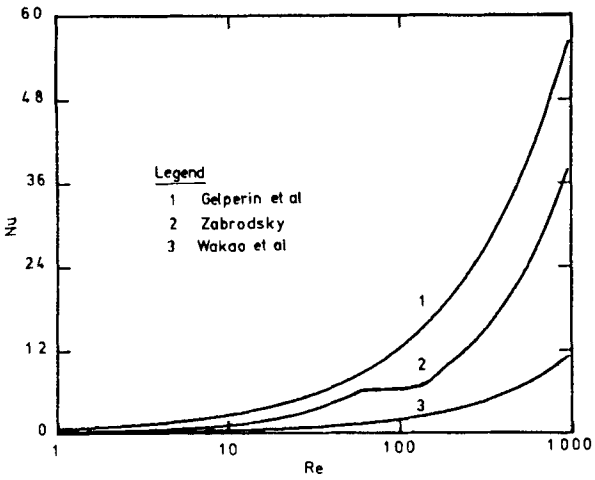

Figure 2. Fluid-to-particle heat transfer.

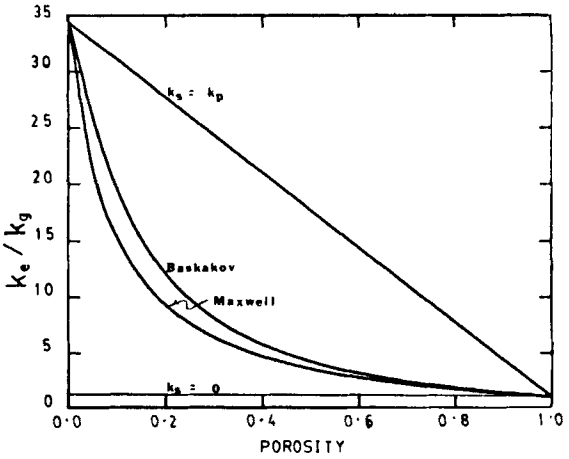

Figure 3. Effective bed conductivity as a function of porosity.

$$\frac{\partial}{\partial t}[(1-\epsilon)\rho_s I_s] + \frac{\partial}{\partial x}[(1-\epsilon)\rho_s I_s U_s] + \frac{\partial}{\partial y}[(1-\epsilon)\rho_s I_s V_s]$$
$$= -P\left\{\frac{\partial}{\partial t}(1-\epsilon) + \frac{\partial}{\partial x}[(1-\epsilon)U_s] + \frac{\partial}{\partial y}[(1-\epsilon)V_s]\right\}$$
$$+ h_v(T_g - T_s) \quad + \frac{\partial}{\partial x}\left[K_s(1-\epsilon)\frac{\partial T_s}{\partial x}\right]$$
$$+ \frac{\partial}{\partial y}\left[K_s(1-\epsilon)\frac{\partial T_s}{\partial y}\right] \quad (13)$$

These equations can be derived from the single-phase equations using the volume averaging technique and approximating some of the resultant surface integrals. Note that the two-phase constitutive equations are different from the single-phase constitutive equations. The gas phase being continuous, its constitutive equations need not be modified. The gas phase is considered to be ideal and its specific heat and thermal conductivity are considered to be constants. For the particulate phase, the specific heat is the same as that for the material of the particles. However, particulate phase heat transfer and interphase heat transfer need further considerations.

INTERPHASE HEAT TRANSFER

The interphase heat transfer term is written in the form $h_v(T_g - T_s)$. The heat transfer occurs primarily through a gas film surrounding the individual particle. We have to use empirical correlations for predicting h_v. There are a large number of correlations available for packed bed gas-solid heat transfer. Some of them may be adapted for fluidized bed conditions. Three correlations from Zabrodsky (1966), Gelperin and Einstein (1971), and Wakao et al. (1978) are shown in Figure 2 for comparison. The former two correlations are suitable for fluidized bed interphase heat transfer. However, these correlations are known to differ from certain experimental data by 100 to 200%. In this study we use correlations taken from Zabrodsky. Also, the interfacial area needed for computing h_v is calculated based on the surface area of equal size spherical particles. It is known that if a hot gas is injected into a cold bed, the gas is quenched by the time it flows past the first row of particles. Simulations using Zabrodsky's correlations predicted the rapid quenching of a hot gas flowing into a cold fluidized bed. Moreover, since the difference in temperature between the phases is not large, the error due to the use of the above correlations can be neglected.

PARTICULATE PHASE HEAT TRANSFER

The heat transfer between the particles poses a major difficulty in formulating the equations. In Eq. 13 it is written in the standard Fourier-law form of $\partial/\partial x(K_s(1-\epsilon)\partial T/\partial x)$, etc. Here K_s is not the conductivity of the material of the particles, but that of a collection of particles considered together as a particulate phase. There is no work known to the authors dealing with the constitutive relation for K_s in a fluidized bed. In the detailed models proposed so far particle-to-particle interaction is usually neglected, assuming point contact between the particles. Bauer and Schlünder (1978) point out that in a packed bed, point contact between the particles, which is usually assumed, does not correspond to the actual situation. In a fluidized bed the situation is slightly different due to the collisions and abrasions among the particles. It will be seen later that these phenomena appear to enhance the particulate phase heat transfer in a fluidized bed. In this study the particulate phase heat transfer is assumed to be significant.

Particle-to-particle transfer is a complex phenomenon, involving contact conductance, conduction through the thin layer of gas sticking to the particles, and radiation. Thus there might be some overlap of mechanisms when empirical correlations are used for calculating interphase heat transfer and particulate phase heat transfer. However, this is not a great concern here since in the near wall region where the particulate phase heat transfer is significant, the interphase heat transfer is insignificant.

There is not a great deal of experimental evidence on the role of particulate phase heat transfer. Conclusions based on the dependence of heat transfer coefficient on the thermal conductivity of the particulate material, K_p, might be misleading. In a model proposed by Botterill (1975), there is a strong dependence of the heat transfer coefficient on the thermal conductivity of the particulate material. Zabrodsky et al. (1978), however, cite experimental data in which fluidization using glass beads and copper shots gave similar heat transfer coefficients. Thus they conclude that at large residence times of particles at the heat transfer surface the influence of K_p is negligible. Although the above assertion may be partly true, the particulate phase heat transfer is by no means insignificant. Wen and Chang, as cited by Botterill (1975), estimate that 10 to 35% of the total heat was transferred by particle-to-particle transfer. Another way of analyzing this mode of transport might be by looking at the effective conductivities of packed beds, as shown in Figure 3. There a correlation due to Baskakov (Gelperin and Einstein 1971) for effective bed conductivity is shown together with the two extreme conditions: $K_s = K_p$ and $K_s = 0$. The fallacy of $K_s = 0$ is obvious. Also shown is a theoretical prediction due to Maxwell (Parrott and Stuckes, 1975) in which he considers the dispersed phase as being covered by a film of continuous phase to get the effective conductivity of the mixture as:

$$\frac{K_{\text{bed}}}{K_g} = \frac{1 + 2K_g/K_s - 2(1-\epsilon)(K_g/K_s - 1)}{1 + K_g/K_s + (1-\epsilon)(K_g/K_s - 1)} \quad (14)$$

Even this model predicts a conductivity smaller than that of Baskakov's. Hence, we conclude that it is essential to consider particulate phase heat transfer and that this mode of transport takes place parallel to the gas phase heat transfer.

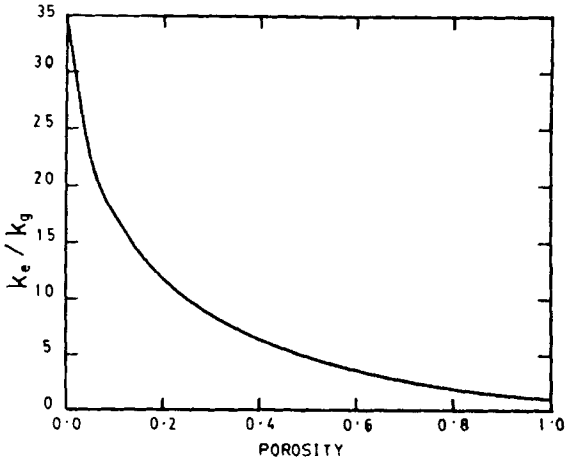

Figure 4. Zehner and Schlünder model for effective radial conductivity of solids in a packed bed.

A good approximation for the particulate phase conductivity is the effective radial thermal conductivity of solids in a packed bed. Nayak and Tien (1978) used a statistical thermodynamic approach to calculate the coordination number distributions and subsequently to calculate the lattice conductivity using a Holm formula. This appears to be a promising approach for modeling fluidized bed particulate heat transfer. However, such an extension is not being attempted here due to the lack of sufficient experimental data to test the model. Here we use a model due to Zehner and Schlünder (Bauer and Schlünder, 1978) for the effective radial conductivity of packings. Neglecting the radiation and Smoluchowski effects, the equations reduce to the following:

$$\frac{K_s}{K_g} = (1 - \sqrt{1-\epsilon}) + \sqrt{1-\epsilon}\left[\phi R + (1-\phi)\frac{\lambda^*_{so}}{\lambda}\right] \quad (15)$$

where

$$\frac{\lambda^*_{so}}{\lambda} = \frac{2}{(1-B/R)}\left[\frac{\frac{B}{R}(R-1)}{(1-B/R)^2} ln\frac{R}{B} - \frac{B-1}{\left(1-\frac{B}{R}\right)} - \frac{B+1}{2}\right]$$

$$R = \frac{K_p}{K_g}$$

$$B = 1.25\left(\frac{1-\epsilon}{\epsilon}\right)^{10/9} \text{ for spheres}$$

$$\phi = 7.26\ 10^{-3}$$

For a glass/air system the above formula is shown in Figure 4. Note that in the operating region of fluidized beds ($\epsilon > 0.4$), K_s is significantly smaller than K_p and is more comparable to K_g. This might be the reason for the apparent absence of the influence of K_p on the heat transfer coefficient as reported by Zabrodsky et al. (1978).

In some of the detailed models it is customary to assume a gap of 0.1 *dp* between the particles and the wall. Although there is an increase in the bed porosity near the wall (Ozkaynak and Chen, 1980; Pillai, 1977), it is not realistic to assume such a gap in a continuum model. For an average bed porosity of 0.45, Gelperin and Einstein (1971) use a wall porosity of 0.476. Such a wall effect is neglected in this study.

NUMERICAL SOLUTION

The set of nonlinear partial differential equations is solved for U_s, U_g, V_s, V_g, ϵ, T_g, T_s and P using the ICE method. (Rivard and Torrey, 1977; Ettehadieh, 1982). Velocities of each phase are centered on the cell boundaries. Quantities such as density, porosity temperature, and pressure are centered at the center of the mesh. Porosities at other locations are found by linear interpolation. Flux

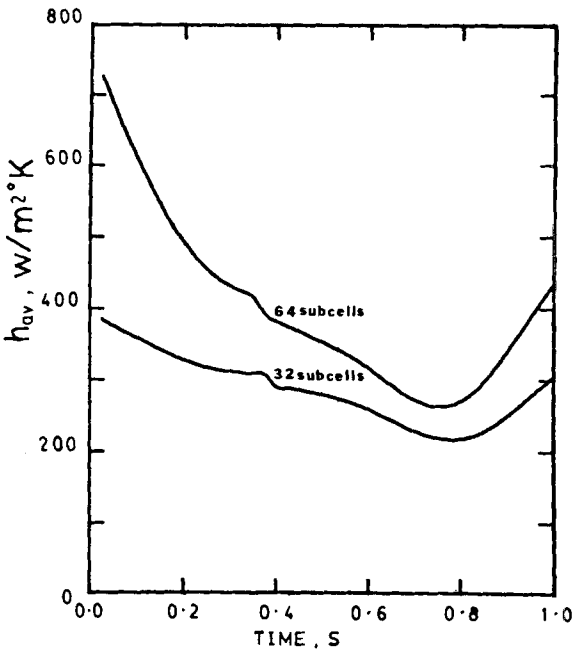

Figure 5. Convergence as the number of subcells is increased.

terms in continuity and momentum equations are full donor-cell differenced. Convective terms in the momentum equations are advanced in time explicitly, whereas all exchanges of mass, momentum, and energy, when they occur, are treated implicitly. The resulting finite difference equations are solved by a combination of point relaxation, Newton's method, and the secant iteration method, without any linearization.

Due to the vigorous circulation of the solids, the bulk of the fluidized bed is practically isothermal. Trial simulations proved that the significant mechanism in the bed-to-wall heat transfer is a transient transport phenomenon very close to the wall. This conforms to the packet model of Mickley and Fairbanks in which they consider the mechanism to be transient conduction to a packet of particles which resides at the heat transfer surface for a short while. Also there is no evidence of a steady-state film of gas or solids near the wall offering a resistance to heat transfer (Saxena et al., 1978). For "capturing" such a transient phenomenon we need much finer computational cells near the wall than those used for the hydrodynamic simulation. Thus for the solution of the energy equations near the wall the regular computational cells are subdivided into subcells. The number of subcells was increased until convergence was obtained, as shown in Figure 5.

The primary goal in this study has been to use the continuum approach to model fluidized bed heat transfer and to establish that the enhancement of the heat transfer coefficient is predictable using simple mechanisms. In addition, we compare our results with the experimental data of Ozkaynak and Chen (1980) for a vertical tube immersed in a uniformly fluidized bed. In a uniformly gas-fluidized bed, bubbles form at random over the distributor plate. However, there is a preferential formation of bubbles near the wall, due to the higher porosity in that region. In the computer simulation, we use a non-uniform gas flow rate at the distributor plate; the gas flow rate near the wall is higher compared to the rest of the bed. However, it was found that the average heat transfer coefficient is insensitive to any particular gas flow rate distribution and that it is sensitive only to the total gas flow rate. A summary of the important simulation conditions which are identical to those of Ozkaynak and Chen's experiment is shown in Table 2.

TABLE 2. COMPUTER SIMULATION CONDITIONS

Particle Diameter (μm)	610
Particle Thermal Conductivity (W/m·K)	0.89
Particle Heat Capacity (J/kg·K)	753.6
Particle Density (kg/m^3)	2.470

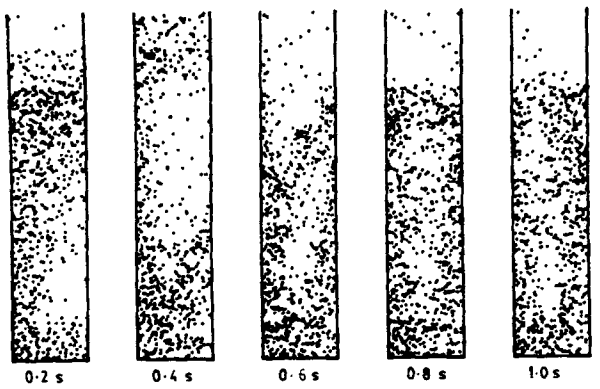

Figure 6. Bubble propagation in the fluidized bed.

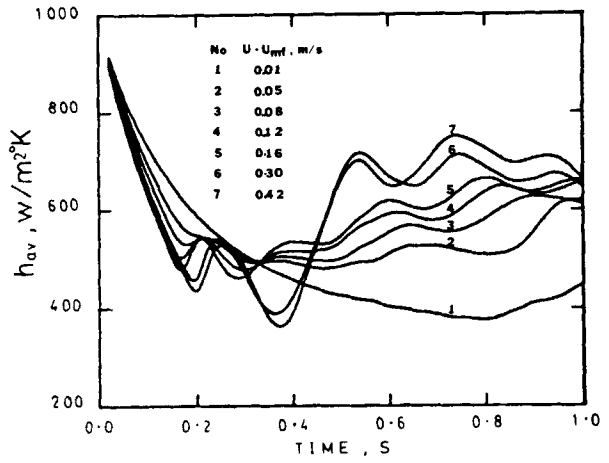

Figure 7. Average bed-to-wall heat transfer coefficients for different gas flow rates.

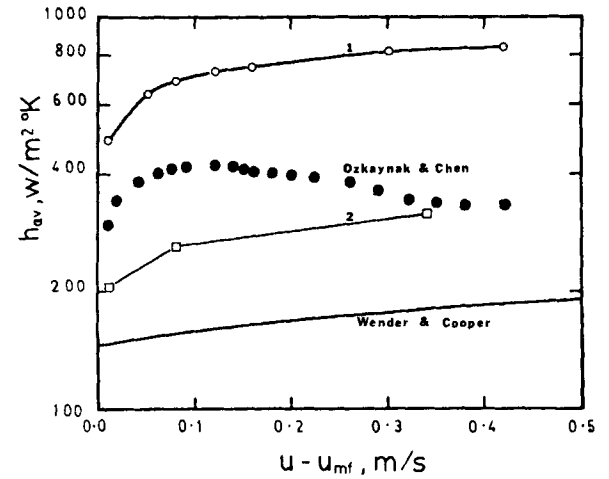

Figure 8. Comparison of average heat transfer coefficients with experimental data.

RESULTS AND DISCUSSIONS

In Figure 6 the bed porosity is shown as a density plot for a typical simulation run. The evolution and propagation of a large bubble in the initial period can be easily seen. This bubble leaves the bed at about 0.4 s. By 0.5 s the start-up transients settle down and thereafter the simulation correctly predicts the propagation of small bubbles (Gidaspow et al., 1983).

In Figure 7 the transient bed averaged heat transfer coefficients for various gas flow rates are shown. The bed averaged wall-to-bed heat transfer coefficient is defined as:

$$h_{av} = \frac{q_{av}}{(T_w - \bar{T})} \tag{16}$$

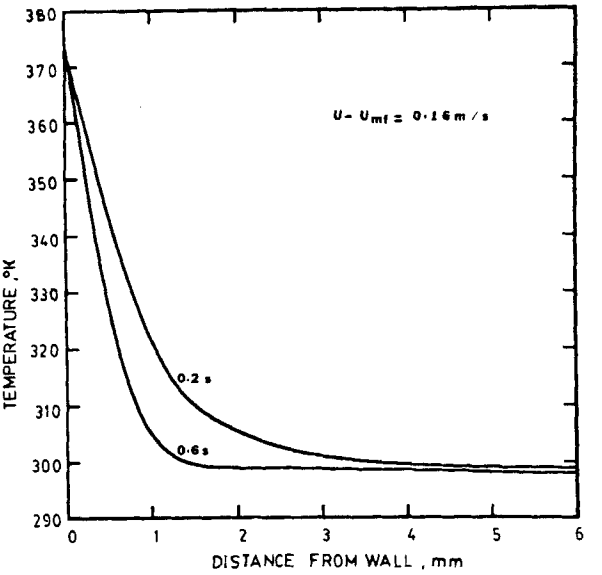

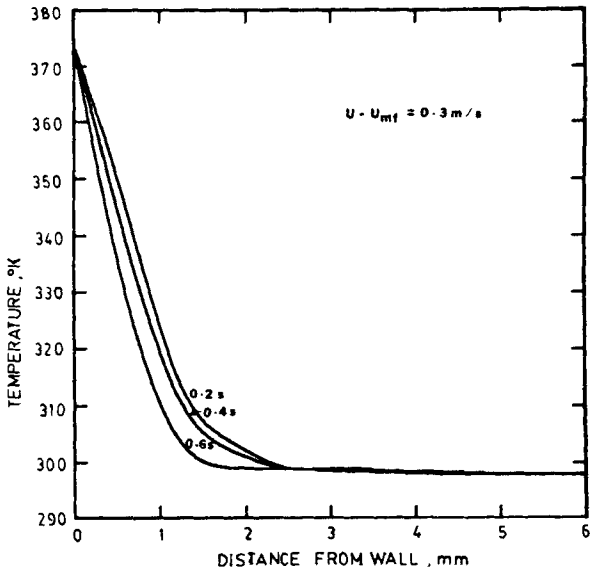

Figure 9. Temperature profile near the wall (0.11 m above the distributor).

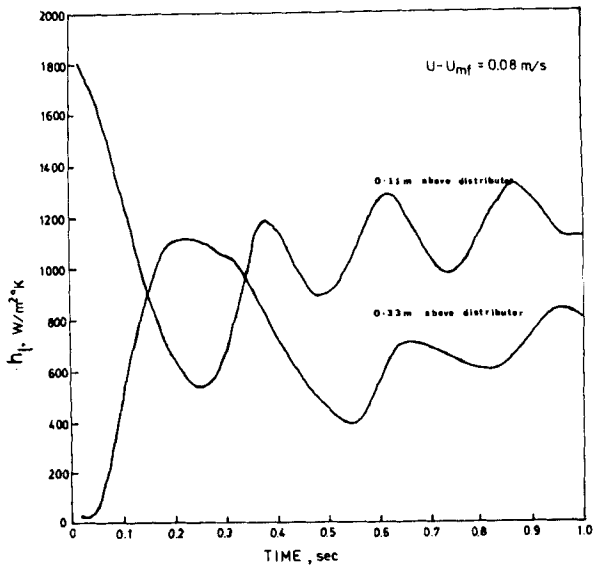

Figure 10. Local heat transfer coefficients at two locations in the bed.

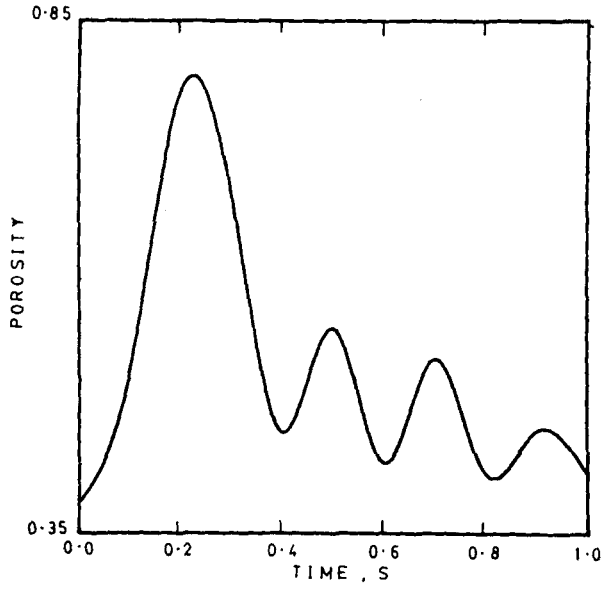

(a)

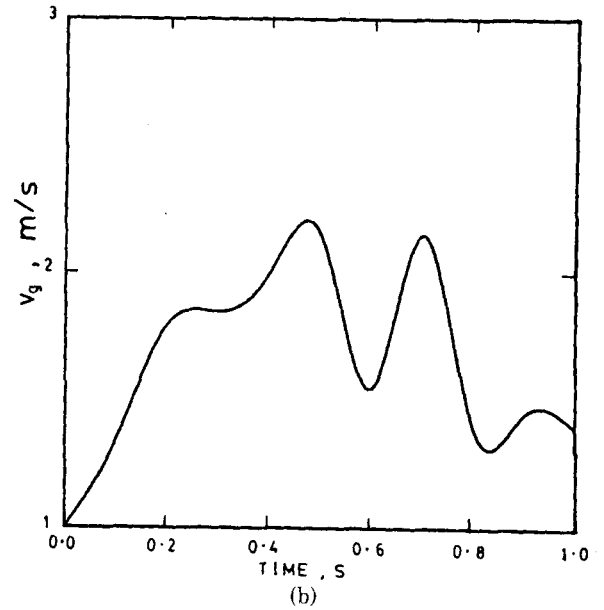

(b)

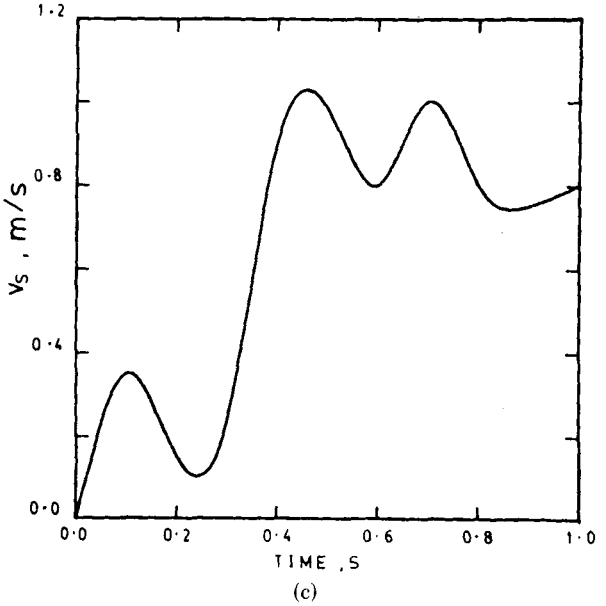

(c)

Figure 11. Porosity (Figure 11a), Gas Velocity (Fig. 11b) and Solid Velocity (Figure 11c) 0.11 m above the distributor at $U - U_{mf} = 0.16$ m/s.

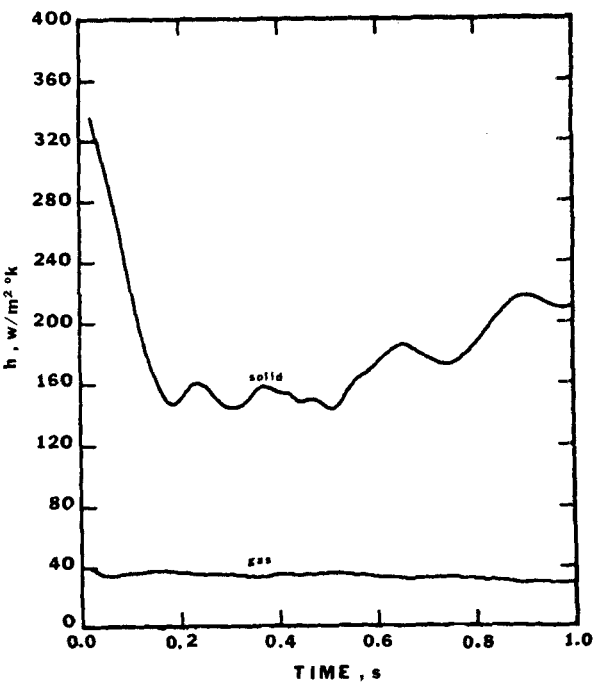

Figure 12. Contributions to heat transfer due to gas phase and particulate phase conduction.

The transient behavior is similar in all the cases. Initially there is a rapid decay in the value of heat transfer coefficient as a temperature profile develops into a nearly static bed. But there are two more phenomena taking place simultaneously in the bed: (1) bed circulation, which disrupts the development of the temperature profile and thus tends to increase the heat transfer coefficient, and (2) growth and propagation of the start-up bubble, which tends to decrease the heat transfer coefficient. The effect of above three mechanisms is more pronounced at higher gas flow rates. The start-up transients disappear by the end of 0.5 s. Hence, we compute the time averaged heat transfer coefficients by integrating the instaneous heat transfer coefficients from 0.5 to 1 s.

In Figure 8 the average heat transfer coefficients are plotted as a function of $U - U_{mf}$, together with experimental data of Ozkaynak and Chen and the predictions of a correlation due to Wender and Cooper (Ozkaynak and Chen, 1980). Curve 1 shows the theoretical predictions when $K_s = K_p$. As expected, the predictions are much higher than the experimental values. However, the theory correctly predicts the sharp rise in the heat transfer coefficients in the beginning, and the leveling off thereafter. Curve 2 shows the theoretical predictions when the Zehner an d Schlünder model for K_s was used. Now the theoretical predictions are reasonably close to the experimental data. It may be that the actual K_s should be higher than that predicted by Zehner and Schlünder model. It must be emphasized that no fitting parameters have been used in the computer simulations. It can be seen that the prediction of the continuum model is superior to the predictions of the correlation.

In Figure 9, the propagation of thermal waves into the bed is shown for different time intervals after startup. Ozkaynak and Chen (1980) observe that the thermal waves penetrate up to a depth of one particle diameter from the wall. In Figures 9a and 9b we observe the same phenomena. It is seen that as time passses the temperature profile becomes steeper. After about 0.4 s the change in the temperature profile is not much; i.e., some kind of a "thermal equilibrium" has been reached near the wall. It is also seen that the behavior of the thermal waves at different gas flow rates is similar.

In Figure 10 the instantaneous local heat transfer coefficients at two different locations in the bed are shown. The effect of the start-up transients is visible at both the locations. At the higher location, which is nearly at the top of the bed, the start-up transients may be seen to leave the bed at about 0.5 s. After this there are

nearly regular fluctuations in the local heat transfer coefficients. In Figure 11, the porosity, axial gas velocity, and axial solid velocity at the lower location are shown. Qualitatively we can correlate the local heat transfer fluctuation to the local porosity fluctuation. To some extent there are some fluctuations in the local gas velocity also, whereas the local solids velocity remains steady. However, from the above figures it is clear that the behavior of the heat transfer coefficient is not amenable to a simple qualitative treatment.

One of the useful aspects of the continuum approach is its ability to provide detailed information on the local behavior of the variables. Figures 9 and 11 are examples. Further, in Figure 12 the contribution to the heat transfer coefficient from the particulate phase and gas phase heat transfer are shown. Such quantities are not easy to measure.

The model can now be extended to fluidized bed combustors. Conservation of species equations for oxygen, carbon monoxide, carbon dioxide, and pollutants such as SO_2 and NO_x, can easily be added to the present computer code. Location of hot spots can be predicted. There is also the potential of extending the model to multiparticle size situations. The presence of fines may alter the heat transfer coefficients to some extent.

NOTATION

B = defined in Eq. 15
C_D = drag coefficient
C_s = specific heat of "packet," J/kg·K
dp = diameter of solid particles, m
g = gravitational force per unit mass, m/s^2
h_i, h_{av}, h_1 = wall-to-bed heat transfer coefficients, $W/m^2 \cdot K$
h_v = interphase heat transfer coefficient, $W/m^3 \cdot K$
I_g = specific internal energy of gas, J/kg
I_s = specific internal energy of solids, J/kg
k_a = thermal conductivity of "packet," W/m·K
K_g = thermal conductivity of gas phase, W/m·K
K_s = thermal conductivity of solid phase, W/m·K
K_p = thermal conductivity of particles, W/m·K
G = modulus of elasticity, particle-to-particle interaction coefficient, N/m^2
Nu = Nusselt number
P = pressure, Pa
q_{av} = average heat transfer to wall, W/m^2
R = defined in Eq. 15
Re_s = solids Reynolds number
T_g = gas phase temperature, K
T_s = solid phase temperature, K
$\overline{T}$ = average bed temperature, K
t = time, s
U_g = lateral gas velocity, m/s
U_s = lateral solid velocity, m/s
U_{mf} = minimum fluidization velocity, m/s
V_g = axial gas velocity, m/s
V_s = axial solid velocity, m/s
x = coordinate in lateral direction, m
y = coordinate in axial direction, m

Greek Letters

β_x and β_y = fluid-particle friction coefficient in the x and y directions, $kg/m^3 \cdot s$
ϵ = gas volume fraction
λ, λ^*_{so} = defined in Eq. 15
τ = solids stress, related to particle-to-particle pressure, N/m^2
τ_p = packet residence time, s
μ_g = gas viscosity, kg/m·s
ρ_g = gas density, kg/m^3
ρ_s, ρ_p = solid and particle densities, kg/m^3
ρ_b = density of "packet"
ϕ_s = sphericity
ϕ = defined in Eq. 15

ACKNOWLEDGMENT

This work was supported by the National Science Foundation under grant No. CPE 8,209,290.

LITERATURE CITED

Adams, R. L., and J. R. Welty, "A Gas Convective Model of Heat Transfer in Large Particle Fluidized Beds," *AIChE J.*, **25**, 395 (1979).

Arastoopour, H., and D. Gidaspow, "Vertical Pneumatic Conveying Using Four Hydrodynamic Models," *I&EC Fundamentals*, **18**, 123 (1979).

Bauer, R., and E. U. Schlünder, "Effective Radial Thermal Conductivity of Packings in Gas Flow. Part II: Thermal conductivity of the packing fraction without gas flow," *Int. Chem. Eng.*, **18**, 189 (1978).

Botterill, J. S. M., *Fluid-Bed Heat Transfer*, Academic Press, New York (1975).

Ettehadieh, B. "Hydrodynamic Analysis of Gas-Solid Fluidized Beds," Ph.D. Dissertation, Illinois Inst. Tech. (1982).

Fanucci, J. B., N. Ness, and R. H. Yen, "On the Formation of Bubbles in Gas-Particulate Fluidized Beds." Part 2, *J. Fluid Mech.*, **94**, 353 (1979).

Galloway, T. R., and B. H. Sage, "A Model of the Mechanism of Transport in Packed, Distended, and Fluidized Beds," *Chem. Eng. Sci.*, **25**, 495 (1970).

Garg, S. K., and J. W. Pritchett, "Dynamics of Gas-Fluidized Beds," *J. Appl. Physics*, **46**, 4493 (1975).

Gelperin, N. I., and V. G. Einstein, "Heat Transfer in Fluidized Beds," *Fluidization*, Academic Press, New York (1971).

Ghate, M., and J. W. Martin, Eds., "Coal Gasification Modeling Workshop Proceedings" *DOE/METC/82-24*, Morgantown, W.VA (Jan., 1982).

Gidaspow, D., "Hyperbolic Compressible Two-Phase Flow Equations Based on Stationary Principles and the Fick's Law," *Two-Phase Transport and Reactor Safety*, T. N. Veziroglu and S. Kakac, Eds. **1**, 283, Hemisphere Pub. Corp., Washington, DC (1978).

Gidaspow, D., and B. Ettehadieh, "Fluidization in Two-Dimensional Beds with a Jet. 2: Hydrodynamic Modeling" *I&EC Fundamentals* **22**, 193 (1983).

Gidaspow, D., Y. C. Seo, and B. Ettehadieh, "Hydrodynamics of Fluidization: Experimental and theoretical bubble sizes in a two-dimensional bed with a jet," *Chem. Eng. Comm.*, **22**, 253 (1983).

Klein, H. H., and M. F. Scharff, "A Time-Dependent Reactive Model of Fluidized Bed Chemical Reactors," *ASME Preprint 82-FE-6* (1982).

Lyczkowski, R. W., et al., "Characteristics and Stability Analyses of Transient One-Dimensional Two-Phase Flow Equations and Their Finite Difference Approximations," *Nuclear Sci. and Eng.* **66**, 378 (1978).

Nayak, A. L., and C. L. Tien, "A Statistical Thermodynamic Theory for Coordination-Number Distribution and Effective Thermal Conductivity of Random Packed Beds," *Int. J. Heat., Mass Transfer* **21**, 669 (1978).

Ozkaynak, T., and J. C. Chen, "Emulsion Phase Residence Time and Its Use in Heat Transfer Models in Fluidized Beds," *AIChE J.*, **26**, 544 (1980).

Parrott, J. E., and A. D. Stuckes, *Thermal Conductivity of Solids*, Methuen, Inc., New York (1975).

Pillai, K. K., "Voidage Variation at the Wall of a Packed Bed of Spheres," *Chem. Eng. Sci.*, **32**, 59 (1977).

Pritchett, J. W., et al., "A Numerical Model of Gas Fluidized Beds," *AIChE Symp. Ser.*, **74**(176), 134 (1978).

Richardson, J. F., and W. N. Zaki, "Sedimentation and Fluidization: Part I," *Trans. Inst. Chem. Eng.*, **32**, 35 (1954).

Rietma, K., and S. M. P. Mutsers, "The Effect of Interparticle Forces on Expansion of a Homogeneous Gas-Fluidized Bed," *Proc. Int. Symp. on Fluidization*, 32 Toulouse, France (1973).

Rivard, W. C., and M. D. Torrey, "K-FIX: A Computer Program for Transient, Two-Dimensional, Two-Fluid Flow," *LA-NUREG-6623*, Los Alamos (1977).

Rowe, P. N., "Drag Forces in a Hydraulic Model of a Fluidized Bed," *Trans. Inst. Chem. Eng.*, **39**, 175 (1961).

Saxena, S. C., et al., "Heat Transfer between a Gas Fluidized Bed and Immersed Tubes," *Advances in Heat Transfer*, **14**, Academic Press, New York (1978).

Scharff et al., "Computer Modeling of Mixing and Agglomeration in Coal Conversion Reactors," *DOE/ET/10,329-1,211* **I, II**, JAYCOR (Feb., 1982).

Schneyer, G. P., et al., "Computer Modeling of Coal Gasification Reactors," *Final Report June 1975-1980, DOE/ET/10,247*, Systems, Science & Software (Apr., 1981).

Wakao, N., S. Kaguei, and T. Funazkri, "Effect of Fluid Dispersion Coefficients on Particle-to-Fluid Heat Transfer Coefficients in Packed Beds," *Chem. Eng. Sci.*, **34**, 325 (1979).
Wen, C. Y., and Y. H. Yu, "Mechanics of Fluidization," *Chem. Eng. Prog. Symp. Ser.*, **62**, 100 (1965).
Wen, C. Y. and Y. H. Yu, *Fluidization*, J. F. Davidson and D. Harrison, Eds., Ch. 16, Academic Press, London (1971).
Zabrodsky, S. S., *Hydrodynamics and Heat Transfer in Fluidized Beds*, M.I.T. Press, Cambridge, MA (1966).
Zabrodsky, S. S., Yu. G. Epanov, and D. M. Galershtein, "On the Dependence of Fluidized Bed-Wall Heat Transfer Coefficients on the Thermal Conductivity and Volumetric Heat Capacity of the Particles," *Fluidization*, Cambridge Univ. Press (1978).

Manuscript received June 3, 1983; revision received September 27, and accepted September 30, 1983.

Evaluation of Changeover Control Policies by Singular Value Analysis—Effects of Scaling

HENRY LAU and K. F. JENSEN

Department of Chemical Engineering and Materials Science
University of Minnesota
Minneapolis, MN 55455

A method for assessing control performance at different operating conditions in a chemical process is developed using singular value analysis. The control potential of the system is established by analyzing the singular values of the steady-state system matrix. Dynamic considerations and interaction analysis can be included in the framework of the method described. The approach enables the process engineer to consider controllability of the process as well as economics in synthesizing a changeover control policy. Singular values depend on the scaling of the system, i.e., the definition of the physical dimensions of the system. The effects of scaling on the analysis are first investigated by scaling the steady-state system matrix with empirical methods, equilibration, and geometric scaling. Using the insights gained from these studies a scaling method, variable normalization and equation equilibration, which is intuitively appealing and suited for the purpose, is devised. Two typical chemical systems, continuous stirred tank reactor and a polymerization reaction system, demonstrate the usefulness of this method.

SCOPE

The design of flexible chemical processes is an important problem facing a process systems engineer. The problem may be structured on three levels: (i) design of regulatory control structures, (ii) design of changeover control policies, and (iii) design of process structures. As one proceeds up the hierarchy, the flexibility of the system increases.

At the bottom level (i), the flexibility lies in the ability of the engineer to select various control interconnections to regulate the process. Several methods are described in the literature for selecting these interconnections (Bristol, 1966; Tung and Edgar, 1977; Witcher and McAvoy, 1977; Morari and Stephanopoulos, 1980; Romagnoli et al., 1980; Govind and Power, 1982; Gagnepain and Seborg, 1982; Lau et al., 1985; Jensen et al., 1982). However, the operating conditions and the process interconnections remain fixed.

At the intermediate level (ii), the operating conditions can be changed if better economic and control performance can be achieved. Consequently, both the control interconnections and the operating conditions can be altered. Algorithms also exist for selecting optimal conditions and for synthesizing the operating route to change from the current conditions to the new conditions (Arkun and Stephanopoulos, 1980; Prett and Gillette, 1980; Bamberger and Isermann, 1978; Garcia and Morari, 1981).

At the highest level (iii), the interconnections between process units become design variables in achieving the desired economic and operational goals. This lends a high degree of flexibility to the process. Morari and his coworkers (Lenhoff and Morari, 1982; Marselle et al., 1982; Morari, 1982, 1983; Morari et al., 1983) have studied this problem extensively, making significant advances toward the integration of process design, process operation, and process control.

In this paper we describe a method for evaluating the controllability of a process by singular value analysis. By plotting contours of the minimum singular value and the condition number of the steady-state system matrix over the feasible region, defined by the state and constraint equations, we can visualize the sensitivity and operability of the process system. This in turn provides a tool for designing changeover control policies. We also demonstrate how the concept of structural controllability of the system as defined by Morari and Stephanopoulos (1980) may be quantified through singular value analysis.

H. Lau is currently with Shell Development Co., Westhollow Research Center, Houston, TX 77001.